

Visual Feedback Leader-following Pose Synchronization: Convergence Analysis

Tatsuya Ibuki, Takeshi Hatanaka, Masayuki Fujita and Mark W. Spong

Abstract—This paper investigates visual feedback pose synchronization on $SE(3)$ in leader-follower type visibility structures. After defining visual robotic networks to be controlled, we propose a visual feedback pose synchronization law combining a vision-based observer with the pose synchronization law presented in our previous works. We then prove that the visual robotic network with the control law achieves visual feedback pose synchronization in the absence of communication or any other measurements of the states. Finally, the validity of the proposed control law is demonstrated through experiments.

I. INTRODUCTION

A mobile sensor network [1], [2] is a network consisting of multiple mobile robots with sensing devices. Mobile sensor networks have potential advantages in performance, robustness against sensor failures and versatility for sensor-driven tasks such as monitoring for environment or infrastructure, search, exploration and mapping, especially in dynamical environments. In operation, each sensor is required to act cooperatively using only limited information. Cooperative control provides methodologies to tackle such distributed control problems [3], where two distinctly different approaches have emerged: an agent taking on leader roles exists or all agents are fully autonomous. This paper focuses on a leader-based cooperative control problem.

Cooperative control problems for mobile sensor networks are formulated as pose (position and attitude) coordination problems [1], [2]. In this paper, we tackle pose synchronization as one of such problems whose objective is to lead agents' poses to a common one by utilizing distributed control strategies. Although pose synchronization laws depending only on relative information with respect to neighboring agents are proposed in [4] and references therein, the way to obtain the relative information is not trivial.

In this paper, we use only vision as a tool to obtain necessary information for pose synchronization. While numerous research works have been devoted to the combination of control techniques with vision [5]-[7], vision-based cooperative control is also tackled [8]-[12]. In one of our previous works [10], we presented a visual feedback pose synchronization law, where we employed a passivity-based visual observer [7] to implement a passivity-based pose synchronization law presented in [4]. However, no theoretical guarantees on synchronization for the integrated system were provided. In [11], we also tackled a visual feedback attitude

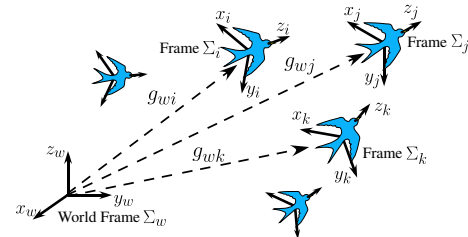


Fig. 1: Rigid Body Motion

synchronization problem which was a partial problem of pose synchronization. Here, we presented a visual feedback attitude synchronization law with theoretical guarantees on attitude synchronization. However, we have not considered position coordination.

In this paper, we investigate a pose synchronization problem for a network of rigid bodies with vision and present a novel vision-based pose synchronization law with theoretical guarantees on synchronization. We first introduce a notion of visual robotic networks to be controlled. After defining visual feedback pose synchronization for the networks, we present a synchronization law consisting of a vision-based observer and synchronization law. We then prove synchronization under appropriate assumptions. Furthermore, from a practical viewpoint, we give another definition of synchronization in order to avoid collisions and guarantee visibility in the final configuration, and also prove synchronization in the sense. The effectiveness of the control scheme is demonstrated through experiments on a planar testbed.

The main contribution of this paper is to present a novel structure incorporating both synchronization control laws and observers into a feedback loop and prove synchronization for the integrated system. Indeed, most of research works similar to our framework take either of two approaches: assuming acquisition of information other than visual data using image processing techniques [12] or treating stability of control and observers separately [8], [10].

II. VISUAL ROBOTIC NETWORK

In this section, we introduce visual robotic networks consisting of the dynamics describing rigid body motion, visibility structures among bodies and visual measurements.

A. Rigid Body Motion

In this paper, we consider a network of n rigid bodies in three-dimensional space (see Fig. 1). Let Σ_w be an inertial coordinate frame and Σ_i , $i \in \mathcal{V} := \{1, \dots, n\}$ body-fixed

T. Ibuki, T. Hatanaka and M. Fujita are with the Department of Mechanical and Control Engineering, Tokyo Institute of Technology, Tokyo 152-8552, JAPAN fujita@ctrl.titech.ac.jp

M. W. Spong is with the Department of Electrical Engineering, University of Texas at Dallas, Richardson, TX 75080 mspong@utdallas.edu

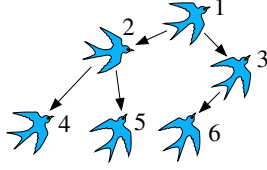


Fig. 2: Leader-follow Type Visibility Structure

coordinate frames. We denote the pose of body i in Σ_w by $(p_{wi}, e^{\hat{\xi}_{wi}\theta_{wi}}) \in SE(3)$ or homogeneous representation

$$g_{wi} = \begin{bmatrix} e^{\hat{\xi}_{wi}\theta_{wi}} & p_{wi} \\ 0 & 1 \end{bmatrix} \in SE(3), \quad i \in \mathcal{V}.$$

Here, $\xi_{wi} \in \mathcal{R}^3$ ($\xi_{wi}^T \xi_{wi} = 1$) and $\theta_{wi} \in \mathcal{R}$ specify the direction and angle of rotation, respectively. For simplicity, we use $\hat{\xi}\theta_{wi}$ to denote $\hat{\xi}_{wi}\theta_{wi}$.

Let us now introduce the velocity of each rigid body to represent rigid body motion of Σ_i relative to Σ_w . We define the body velocity of body i relative to Σ_w as $V_{wi}^b = [(v_{wi}^b)^T (\omega_{wi}^b)^T]^T := (g_{wi}^{-1} \dot{g}_{wi})^\vee \in \mathcal{R}^6$, where $v_{wi}^b \in \mathcal{R}^3$ and $\omega_{wi}^b \in \mathcal{R}^3$ represent the linear and angular velocities. Then, rigid body motion is represented by the kinematic model

$$\dot{g}_{wi} = g_{wi} \hat{V}_{wi}^b, \quad i \in \mathcal{V}. \quad (1)$$

We denote the pose of a frame Σ_j relative to Σ_i as $g_{ij} = (p_{ij}, e^{\hat{\xi}_{ij}\theta_{ij}}) := g_{wi}^{-1} g_{wj} \in SE(3)$. Then, differentiating g_{ij} with respect to time yields the body velocity of the relative rigid body motion

$$V_{ij}^b := (g_{ij}^{-1} \dot{g}_{ij})^\vee = -\text{Ad}_{(g_{ij}^{-1})} V_{wi}^b + V_{wj}^b, \quad (2)$$

where $\text{Ad}_{(g_{ij}^{-1})} \in \mathcal{R}^{6 \times 6}$ is the adjoint transformation associated with g_{ij} [13].

B. Visibility Structure

We describe visibility structures among rigid bodies. Throughout this paper, we assume each body has vision to capture other visible bodies. A set $\mathcal{E} \subset \mathcal{V} \times \mathcal{V}$ is defined so that $(j, i) \in \mathcal{E}$ means body j is visible from body i . We next define the set of visible bodies from body i as

$$\mathcal{N}_i := \{j \in \mathcal{V} \mid (j, i) \in \mathcal{E}\}, \quad i \in \mathcal{V}. \quad (3)$$

Let us now make the following assumptions on the visibility structure.

Assumption 1: (Leader-follower Type Visibility Structure)

- $\mathcal{N}_1 = \emptyset$.
- $|\mathcal{N}_i| = 1$ and \mathcal{N}_i is fixed for all $i \in \mathcal{V} \setminus \{1\}$.
- $\forall i \in \mathcal{V} \setminus \{1\}, \exists v_1, \dots, v_r \in \mathcal{V}$ s.t. $v_1 = 1, v_r = i$ and $(v_k, v_{k+1}) \in \mathcal{E} \forall k \in \{1, \dots, r-1\}$.

Here, $|\mathcal{N}_i|$ represents the number of components of \mathcal{N}_i . Assumption 1 means that visibility structures have leader-follower structures (see Fig. 2).

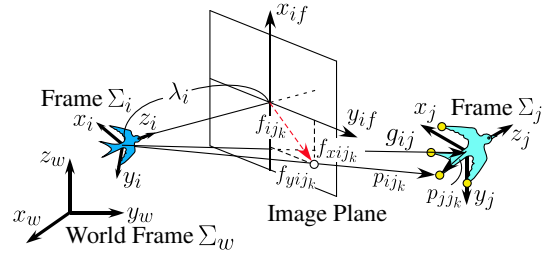


Fig. 3: Perspective Projection Model

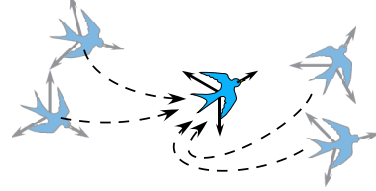


Fig. 4: Pose Synchronization

C. Visual Measurement

Suppose that each rigid body j has m ($m \geq 4$) feature points, whose positions relative to Σ_j are denoted by $p_{jjk} \in \mathcal{R}^3$, $k \in \{1, \dots, m\}$. A coordinate transformation yields the positions of feature points relative to frame Σ_i as $p_{ijk} = g_{ij} p_{jjk}$, where p_{ijk} and p_{jjk} should be regarded as $[p_{ijk}^T \ 1]^T$ and $[p_{jjk}^T \ 1]^T$, respectively [13].

Let us now consider visual measurements of each rigid body. We denote the k -th feature point on the image plane as $f_{ijk} \in \mathcal{R}^2$, $k \in \{1, \dots, m\}$. Then, by perspective projection (Fig. 3 [13]), f_{ijk} is given by $f_{ijk} = (\lambda_i / z_{ijk}) [x_{ijk} \ y_{ijk}]^T$, where $p_{ijk} = [x_{ijk} \ y_{ijk} \ z_{ijk}]^T$ and $\lambda_i \in \mathcal{R}$ is a focal length of body i 's vision. We assume each body can extract the feature points of visible bodies from image data. Visual measurements of body i is thus defined as

$$f_i := (f_{ij})_{j \in \mathcal{N}_i}, \quad i \in \mathcal{V}, \quad (4)$$

where $f_{ij} := [f_{ij1}^T \ \dots \ f_{ijm}^T]^T \in \mathcal{R}^{2m}$.

Hereafter, the aggregate system consisting of n rigid bodies with kinematic model (1), visibility structures (3) satisfying Assumption 1 and visual measurements (4) is called visual robotic network Σ .

III. VISUAL FEEDBACK POSE SYNCHRONIZATION

In this section, we present a visual feedback pose synchronization law and prove that the control law on the visual robotic network Σ achieves synchronization.

A. Definition of Visual Feedback Pose Synchronization

The goal of this paper is to design a body velocity input V_{wi}^b so that the visual robotic network Σ achieves visual feedback pose synchronization defined below.

Definition 1: A visual robotic network Σ is said to achieve visual feedback pose synchronization, if V_{wi}^b depends only on visual measurements (4) and

$$\lim_{t \rightarrow \infty} \Pi (g_{wi}^{-1} g_{wj}) = 0 \quad \forall i, j \in \mathcal{V}. \quad (5)$$

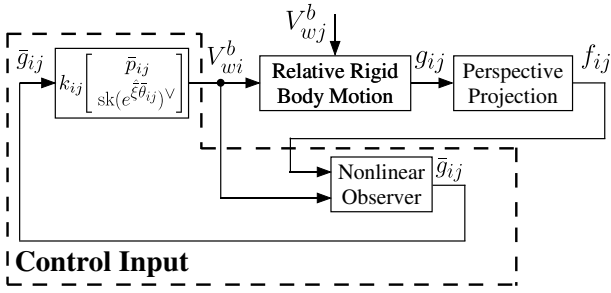


Fig. 5: Visual Feedback Pose Synchronization Law

Here, $\Pi(g_{wi}) := (1/2)\|p_{wi}\|^2 + \phi(e^{\hat{\xi}\theta_{wi}}) \geq 0$, $\phi(e^{\hat{\xi}\theta_{wi}}) := (1/2)\text{tr}(I_3 - e^{\hat{\xi}\theta_{wi}}) \geq 0$ is the energy of a pose error (I_n is $n \times n$ identity matrix). By the definition, $\Pi(g_{wi}) = 0$ if and only if $g_{wi} = I_4$.

Equation (5) implies that poses of all rigid bodies asymptotically converge to a common value (see Fig. 4). Unlike [4] premising the measurement of g_{ij} , the objective is to present a velocity law using only visual measurements (4).

B. Visual Feedback Pose Synchronization Law

We propose the following control law.

$$\text{Controller: } V_{wi}^b = k_{ij} \begin{bmatrix} \bar{p}_{ij} \\ \text{sk}(e^{\hat{\xi}\theta_{ij}})^\vee \end{bmatrix}, \quad (6a)$$

$$\text{Observer} \begin{cases} \bar{V}_{ij}^b := (\bar{g}_{ij}^{-1} \dot{\bar{g}}_{ij})^\vee = -\text{Ad}_{(\bar{g}_{ij}^{-1})} V_{wi}^b + u_{ij}, & (6b) \\ u_{ij} = k_{eij} \left(e_{eij} - \text{Ad}_{(e^{-\hat{\xi}\theta_{ij}})} \begin{bmatrix} \bar{p}_{ij} \\ \text{sk}(e^{\hat{\xi}\theta_{ij}})^\vee \end{bmatrix} \right), & (6c) \end{cases}$$

$j \in \mathcal{N}_i, i \in \mathcal{V}$,

where $k_{ij}, k_{eij} \in \mathcal{R}$ are positive gains and $\text{sk}(e^{\hat{\xi}\theta_{ij}}) \in \mathcal{R}^{3 \times 3}$ is the skew-symmetric part of the matrix $e^{\hat{\xi}\theta_{ij}}$. The block diagram of control law (6) is shown in Fig. 5. Velocity input (6a) is the same as that in [4] except for using $\bar{g}_{ij} = (\bar{p}_{ij}, e^{\hat{\xi}\theta_{ij}}) \in SE(3)$ instead of g_{ij} . Here, \bar{g}_{ij} is an estimate of relative pose g_{ij} given by observer (6b), (6c).

Equation (6b) simulates relative rigid body motion (2) by using the estimate \bar{g}_{ij} as its state. Here, $u_{ij} \in \mathcal{R}^6$ is an external input to be determined so that the estimated values \bar{g}_{ij} and \bar{V}_{ij}^b are driven to their actual values. Equation (6c) determines u_{ij} , where $e_{eij} := [p_{eij}^\top (\text{sk}(e^{\hat{\xi}\theta_{eij}})^\vee)^\top]^\top \in \mathcal{R}^6$ with $g_{eij} := \bar{g}_{ij}^{-1} g_{ij}$. $g_{eij} = (p_{eij}, e^{\hat{\xi}\theta_{eij}}) \in SE(3)$ is the estimation error between the actual relative pose g_{ij} and its estimate \bar{g}_{ij} , and e_{eij} is its vector representation. Note that $e_{eij} = 0$ if and only if $g_{eij} = I_4$ as long as $|\theta_{eij}| < \pi$, namely, if the estimation error vector is equal to zero, then the estimated relative pose \bar{g}_{ij} equals to the actual one g_{ij} . Differentiating g_{eij} with respect to time and utilizing (2) and (6b), we get the following estimation error system.

$$V_{eij}^b := (g_{eij}^{-1} \dot{g}_{eij})^\vee = -\text{Ad}_{(g_{eij}^{-1})} u_{ij} + V_{wj}^b. \quad (7)$$

In (6c), e_{eij} and hence the present control law (6) can be calculated only by visual measurements f_{ij} in the absence

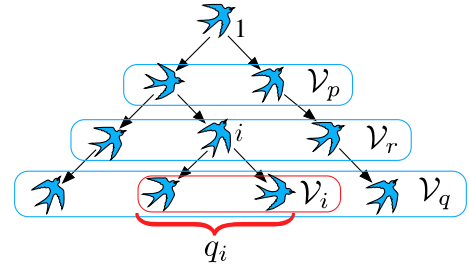


Fig. 6: Definition of Rigid Body Sets

of communication or any other measurements of the states (refer to [7]).

C. Convergence Analysis

In this subsection, we prove that control law (6) on the visual robotic network Σ achieves (5).

First of all, we define the controll error $g_{cij} = (p_{cij}, e^{\hat{\xi}\theta_{cij}}) \in SE(3)$ as $g_{cij} := \bar{g}_{ij}$ (this definition is modified in the following section) and control error vector $e_{eij} \in \mathcal{R}^6$ as $e_{eij} := [p_{cij}^\top (\text{sk}(e^{\hat{\xi}\theta_{cij}})^\vee)^\top]^\top$. Note that $e_{eij} = 0$ if and only if $g_{cij} = I_4$ ($\bar{g}_{ij} = I_4$) as long as $|\theta_{cij}| < \pi$. Since $g_{cij} = \bar{g}_{ij}$, the dynamics of g_{cij} is

$$V_{cij}^b := (g_{cij}^{-1} \dot{g}_{cij})^\vee = -\text{Ad}_{(g_{cij}^{-1})} V_{wi}^b + u_{ij}. \quad (8)$$

This system is the same as (6b) and called control error system. Note that if $g_{cij} = I_4$, $g_{eij} = I_4$, $j \in \mathcal{N}_i \forall i \in \mathcal{V}$, then visual feedback pose synchronization is achieved. Moreover, we use the following notations for leader-follower type visibility structures (see Fig. 6).

$$\begin{cases} \mathcal{V}_p := \{i \in \mathcal{V} \mid 1 \in \mathcal{N}_i\} \\ \mathcal{V}_q := \{i \in \mathcal{V} \mid i \notin \mathcal{N}_j \forall j \in \mathcal{V}\} \\ \mathcal{V}_r := \mathcal{V} \setminus (\{1\} \cup \mathcal{V}_p \cup \mathcal{V}_q) \\ \mathcal{V}_i := \{j \in \mathcal{V}_q \mid \exists v_1, \dots, v_r \in \mathcal{V} \text{ s.t. } v_1 = i, v_r = j \\ \text{and } (v_k, v_{k+1}) \in \mathcal{E} \forall k \in \{1, \dots, r-1\}\} \end{cases}$$

We consider the total system combining control error system (8) with estimation error system (7) as

$$\begin{bmatrix} V_{cij}^b \\ V_{eij}^b \end{bmatrix} = \begin{bmatrix} -\text{Ad}_{(g_{cij}^{-1})} & I_6 \\ 0 & -\text{Ad}_{(g_{eij}^{-1})} \end{bmatrix} \begin{bmatrix} V_{wi}^b \\ u_{ij} \end{bmatrix} + \begin{bmatrix} 0 \\ V_{wj}^b \end{bmatrix}. \quad (9)$$

In this paper, the collection of the combining system (9) for $j \in \mathcal{N}_i, i \in \mathcal{V}$ with control law (6) is called collective error system Σ_{col} , whose state, denoted by $x_e \in \mathcal{R}^{12(n-1)}$, is given by the stuck vector of $e_{ij} := [e_{cij}^\top e_{eij}^\top]^\top \in \mathcal{R}^{12}$, $j \in \mathcal{N}_i, i \in \mathcal{V}$.

We show that control law (6) on the visual robotic network Σ achieves visual feedback pose synchronization (5).

Theorem 1: Suppose that the leader's velocity is zero ($V_{w1}^b = 0$). Then, control law (6) on the visual robotic network Σ achieves visual feedback pose synchronization at least locally if

$$\begin{cases} k_{jk} < \frac{2k_{ij}k_{eij}}{k_{ij}+k_{eij}}, & k \in \mathcal{N}_j, j \in \mathcal{N}_i, i \in \mathcal{V}_q \\ k_{jk} < \frac{2k_{ij}k_{eij}}{k_{ij}+2k_{eij}}, & k \in \mathcal{N}_j, j \in \mathcal{N}_i, i \in \mathcal{V}_r \end{cases}. \quad (10)$$

Proof: From the definition of x_e , if the equilibrium point $x_e = 0$ is asymptotically stable, then local visual feedback pose synchronization is achieved. It is thus sufficient to prove asymptotic stability of $x_e = 0$ for the collective error system Σ_{col} . This can be proved by differentiating the following Lyapunov function candidate with respect to time and utilizing completing square.

$$U := \sum_{i=2}^n \sum_{j \in \mathcal{N}_i} q_i (\Pi(g_{cij}) + \Pi(g_{eij})) \geq 0.$$

Here, $q_i \in \{1, 2, 3, \dots\}$ is $|\mathcal{V}_i|$ for $i \in \mathcal{V} \setminus \mathcal{V}_q$ and $q_i = 1$ for $i \in \mathcal{V}_q$ (Fig. 6). Note that $U = 0$ if and only if $g_{cij} = I_4$, $g_{eij} = I_4$ (i.e. $e_{cij} = 0$, $e_{ij} = 0$ as long as $|\theta_{cij}| < \pi$, $|\theta_{eij}| < \pi$), $j \in \mathcal{N}_i \forall i \in \mathcal{V}$ and otherwise $U > 0$. ■

Gain conditions (10) imply that if the backward rigid bodies move fast, then visual feedback pose synchronization is achieved [11].

It should be noted that Theorem 1 proves synchronization for the system integrating the observers instead employing certainly equivalence principle. It is well known in robot control that proving stability for the integrated system in observer-based control strategies is much more difficult than the individual control and estimation problems even for a single passive system [14]. It should be also true or might be much harder for synchronization since it is required to estimate not their own but the other individuals' information only from relative measurements [15].

We assume $V_{w1}^b = 0$ in Theorem 1. However, even if $V_{w1}^b \neq 0$, it is expected for followers to track the leader and achieve flocking-like behavior. Analyzing the tracking performance in the presence of V_{w1}^b is left as a future work of this paper. The theory of L_2 -gain analysis might be helpful to tackle the problem as in [7], where the authors investigate a vision-based target tracking problem. Also, visibility maintenance is not considered in this work. This problem is also our future work.

IV. EXTENDED RESULTS OF VISUAL FEEDBACK POSE SYNCHRONIZATION

In the previous section, we present a control law to achieve visual feedback pose synchronization in the sense of (5). However, from the practical point of view, the results have problems: (i) With control law (6), all rigid bodies would stop in the final configuration though it is required for bodies to move in the desired direction while achieving pose synchronization. (ii) Following the definition of (5), after synchronization, bodies collide with each other and perspective projection makes no sense. We thus investigate extended versions of synchronization to overcome the problems.

A. Visual Feedback Pose Synchronization with Desired Velocities

In this subsection, we add a common desired velocity to all rigid bodies in order to overcome problem (i).

Suppose that all rigid bodies have a common desired velocity $V_d \in \mathcal{R}^6$ and each body knows the velocity in its

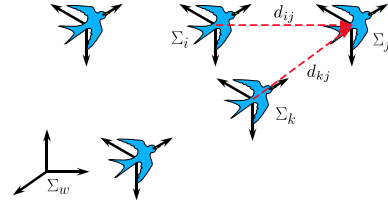


Fig. 7: Virtual Visual Feedback Pose Synchronization

own coordinate frame (i.e. $\text{Ad}_{(e^{-\hat{\xi}\theta_{wi}})} V_d$). Let us fix the form of each body velocity as

$$V_{wi}^b = \tilde{V}_{wi}^b + \text{Ad}_{(e^{-\hat{\xi}\theta_{wi}})} V_d$$

for some \tilde{V}_{wi}^b . Then, relative rigid body motion (2) can be represented by

$$V_{ij}^b = -\text{Ad}_{(g_{ij}^{-1})} \tilde{V}_{wi}^b + \tilde{V}_{wj}^b. \quad (11)$$

Also, estimation error system (7) is derived as

$$V_{eij}^b = -\text{Ad}_{(g_{eij}^{-1})} u_{ij} + \tilde{V}_{wj}^b. \quad (12)$$

Equations (11) and (12) mean that control and estimation error systems do not change except for using \tilde{V}_{wi}^b instead of V_{wi}^b . Therefore, we propose the following control law.

$$\text{Controller: } V_{wi}^b = k_{ij} \begin{bmatrix} \bar{p}_{ij} \\ \text{sk}(e^{\hat{\xi}\bar{\theta}_{ij}})^\vee \end{bmatrix} + \text{Ad}_{(e^{-\hat{\xi}\theta_{wi}})} V_d,$$

$$\text{Observer } \begin{cases} \bar{V}_{ij}^b := (\bar{g}_{ij}^{-1} \dot{\bar{g}}_{ij})^\vee = -\text{Ad}_{(\bar{g}_{ij}^{-1})} \tilde{V}_{wi}^b + u_{ij}, \\ u_{ij} = k_{eij} \left(e_{eij} - \text{Ad}_{(e^{-\hat{\xi}\bar{\theta}_{ij}})} \begin{bmatrix} \bar{p}_{ij} \\ \text{sk}(e^{\hat{\xi}\bar{\theta}_{ij}})^\vee \end{bmatrix} \right), \\ j \in \mathcal{N}_i, i \in \mathcal{V}, \end{cases} \quad (13)$$

Then, we have the following corollary which can be proved by the same way as Theorem 1.

Corollary 1: Suppose that the leader's body velocity is $\text{Ad}_{(e^{-\hat{\xi}\theta_{w1}})} V_d$. Then, control law (13) on the visual robotic network Σ achieves visual feedback pose synchronization at least locally if gain conditions (10) are satisfied.

B. Visual Feedback Pose Synchronization with Biases

In this subsection, we add biases to pose synchronization in order to overcome problem (ii) according to [16].

We define a virtual relative pose $\tilde{g}_{ij} \in SE(3)$ as

$$\tilde{g}_{ij} := \begin{bmatrix} e^{\hat{\xi}\bar{\theta}_{ij}} & p_{ij} - d_{ij} \\ 0 & 1 \end{bmatrix}, \quad i, j \in \mathcal{V},$$

where $d_{ij} \in \mathcal{R}^3$, $i, j \in \mathcal{V}$ are constant biases such that each rigid body guarantees collision avoidance and visibility to neighbors in the final configuration. We assume each body has biases relative to its neighbors d_{ij} , $j \in \mathcal{N}_i$. Then, from Assumption 1, all biases d_{ij} , $i, j \in \mathcal{V}$ are determined (e.g. $d_{ji} = -d_{ij}$, $d_{ik} = d_{ij} + d_{jk}$). According to the modification, an extended version of pose synchronization called virtual visual feedback pose synchronization is defined below.

Definition 2: A visual robotic network Σ is said to achieve virtual visual feedback pose synchronization, if V_{wi}^b depends only on visual measurements (4) and

$$\lim_{t \rightarrow \infty} \Pi(\tilde{g}_{ij}) = 0, \quad \forall i, j \in \mathcal{V}. \quad (14)$$

Equation (14) implies that orientations of all rigid bodies asymptotically converge to a common value and positions form the desired configuration (Fig. 7).

We propose the following control law to achieve (14).

$$\begin{aligned} \text{Controller: } V_{wi}^b &= k_{ij} \begin{bmatrix} \bar{p}_{ij} - d_{ij} + \hat{d}_{ij} \text{sk}(e^{\hat{\xi}\bar{\theta}_{ij}})^\vee \\ \text{sk}(e^{\hat{\xi}\bar{\theta}_{ij}})^\vee \end{bmatrix}, \\ \text{Observer } \begin{cases} \bar{V}_{ij}^b := (\bar{g}_{ij}^{-1} \dot{\bar{g}}_{ij})^\vee = -\text{Ad}_{(\bar{g}_{ij}^{-1})} V_{wi}^b + u_{ij}, \\ u_{ij} = k_{eij} \left(e_{eij} - \text{Ad}_{(e^{-\hat{\xi}\bar{\theta}_{ij}})} \begin{bmatrix} \bar{p}_{ij} - d_{ij} \\ \text{sk}(e^{\hat{\xi}\bar{\theta}_{ij}})^\vee \end{bmatrix} \right), \end{cases} \\ & j \in \mathcal{N}_i, i \in \mathcal{V}. \quad (15) \end{aligned}$$

Accordingly, the definition of the controll error g_{cij} is replaced by $g_{cij} := g_{dij}^{-1} \bar{g}_{ij}$ with the desired relative pose

$$g_{dij} := \begin{bmatrix} I_3 & d_{ij} \\ 0 & 1 \end{bmatrix} \in SE(3).$$

Here, g_{cij} represents the error between the estimated relative pose \bar{g}_{ij} and the desired one g_{dij} . Since d_{ij} is constant, the control error system is represented as

$$V_{cij}^b = -\text{Ad}_{(g_{cij}^{-1})} \text{Ad}_{(g_{dij}^{-1})} V_{wi}^b + u_{ij}.$$

In summary, the total system combining the control error system with the estimation system is reformulated as

$$\begin{bmatrix} V_{cij}^b \\ V_{eij}^b \end{bmatrix} = \begin{bmatrix} -\text{Ad}_{(g_{cij}^{-1})} & I_6 \\ 0 & -\text{Ad}_{(g_{eij}^{-1})} \end{bmatrix} \begin{bmatrix} \text{Ad}_{(g_{dij}^{-1})} V_{wi}^b \\ u_{ij} \end{bmatrix} + \begin{bmatrix} 0 \\ V_{wj}^b \end{bmatrix}. \quad (16)$$

Then, we also build the collective error system Σ_{colv} by replacing (9) by (16) whose state is x_e defined the same as Σ_{col} . Since Σ_{col} and Σ_{colv} differ only in the velocity input, we have the following corollary similarly to Theorem 1.

Corollary 2: Suppose that the leader's velocity is zero ($V_{w1}^b = 0$). Then, control law (15) on the visual robotic network Σ achieves virtual visual feedback pose synchronization at least locally if

$$\begin{cases} I_6 - D_{i1} > 0, \quad i \in \mathcal{V}_p, \\ k_{jk} < \frac{2k_{ij}k_{eij}}{k_{ij} + k_{eij}}, \quad k \in \mathcal{N}_j, \quad j \in \mathcal{N}_i, \quad i \in \mathcal{V}_q, \\ \begin{cases} k_{jk} < 2k_{eij}, \\ k_{jk}(k_{eij}I_6 + k_{ij}(I_6 - D_{ij})) < 2k_{ij}k_{eij}(I_6 - D_{ij}), \end{cases} \\ k \in \mathcal{N}_j, \quad j \in \mathcal{N}_i, \quad i \in \mathcal{V}_r, \end{cases} \quad (17)$$

where $D_{ij} := (1/2)\text{Ad}_{(g_{dij}^T)}\text{Ad}_{(g_{dij})}$.

Proof: Corollary 2 can be proved by using the same Lyapunov function candidate and almost the same approach as in Theorem 1. The difference is as follows.

$$\begin{aligned} e_{eij}^T \text{Ad}_{(e^{\hat{\xi}\theta_{eij}})} V_{wj}^b &= k_{jk} e_{eij}^T \text{Ad}_{(e^{\hat{\xi}\theta_{eij}})} \text{Ad}_{(g_{djk})} e_{cjk} \\ &= \frac{1}{2} k_{jk} \left(\|\text{Ad}_{(g_{djk})} e_{cjk}\|^2 + \|e_{eij}\|^2 \right. \\ &\quad \left. - \left\| \text{Ad}_{(g_{djk})} e_{cjk} - \text{Ad}_{(e^{-\hat{\xi}\theta_{eij}})} e_{eij} \right\|^2 \right). \end{aligned}$$

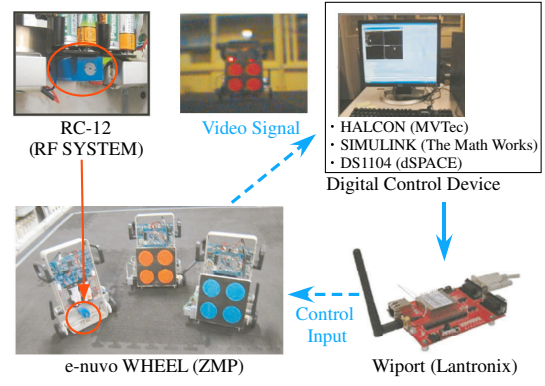


Fig. 8: Experimental Environment

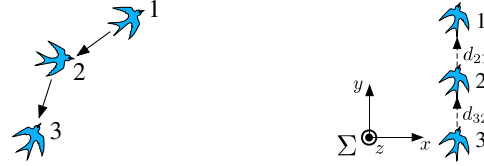


Fig. 9: Visibility Graph in Experiment

Due to the difference, conditions (10) is replaced by (17). ■

It is noted that conditions (14) are reduced to linear matrix inequalities on control gains. Thus, we can find gains by using existing solvers if it is feasible.

V. EXPERIMENT

In this section, we demonstrate the effectiveness of the proposed control laws through experiments on a planar testbed.

In this experiment, we use wheeled mobile robots as rigid bodies. Each robot has a wireless on-board camera. We attach a plate with four colored circles to each robot in order to improve accuracy of extracting feature points. We also use an overhead camera attached above the robots to measure the actual poses of robots. Transmitted video signals are loaded into PC and the control law is calculated in real time. Then the control inputs are sent to robots via embedded wireless communication devices. Since the robot has underactuated characteristics, a local controller due to Astolfi [17] is embedded to the microcomputer so that it tracks to any desirable position and orientation, and we use the present velocity control law as a high-level controller generating desirable positions and orientations. This experimental schematic is shown in Fig. 8. Refer to [11] for the detail of each device.

We use the visibility structure depicted in Fig. 9. We let gains be $k_{e21} = k_{e32} = 15$, $k_{21} = k_{32} = 1$ satisfying (17) and biases be $d_{21} = d_{32} = [0 \ 0.35 \ 0]^T$ [m] (Fig. 10). Initial conditions are set as

$$\begin{aligned} p_{w1}(0) &= [0.707 \ 0.753 \ 0]^T, & \xi_{\theta_{w1}}(0) &= [0 \ 0 \ 2.552]^T, \\ p_{w2}(0) &= [1.157 \ 0.384 \ 0]^T, & \xi_{\theta_{w2}}(0) &= [0 \ 0 \ 2.663]^T, \\ p_{w3}(0) &= [1.510 \ 0.139 \ 0]^T, & \xi_{\theta_{w3}}(0) &= [0 \ 0 \ 2.055]^T, \end{aligned}$$

where units of positions and orientations are [m] and [rad], respectively. Finally, we set the desired common velocity as

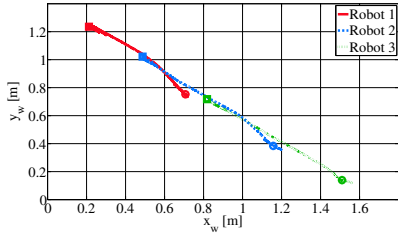


Fig. 11: Positions in Σ_w

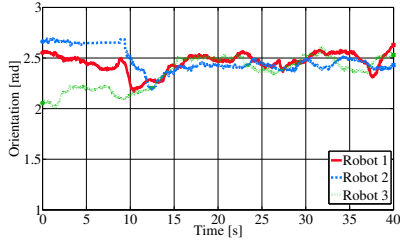


Fig. 12: Rotation Angles in Σ_w

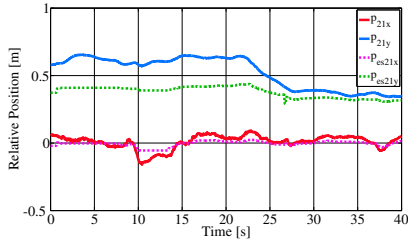


Fig. 13: Actual (Measured) and Estimated Relative Positions between 2 and 1

0 and the leader's body velocity V_{w1}^b as

$$V_{w1}^b = \begin{cases} [0 \ 0.05 \ 0 \ 0 \ 0 \ 0.1]^T & t \in [10, 15) \\ [0 \ 0.05 \ 0 \ 0 \ 0 \ 0]^T & t \in [15, 25) \\ 0 & t \in [25, 40] \end{cases}.$$

Velocity law (15) is applied at 10 [s].

The experimental results are shown in Figs. 11-13. Fig. 11 illustrates the trajectories of the robots on 2-dimensional plane, Fig. 12 time responses of actual orientations and Fig. 13 the actual and estimated positions of robot 1 relative to 2 (we get almost the same results of robot 2 relative to 3). We see from Figs. 11 and 13 that the desired relative positions are achieved at around 27 [s] and the error between actual and estimated pose is small enough to achieve a stable pose. Moreover, Fig. 12 shows that all orientations converge to almost a common value (robot 1's value). The results mean that the proposed control law (15) achieves virtual visual feedback pose synchronization and thus the synchronization law works successfully.

It is possible to download the movie of this experiment from <http://www.fl.ctrl.titech.ac.jp/researches/movie/movie2/vfps.wmv>.

VI. CONCLUSIONS

In this paper, we have investigated pose synchronization by using visual information as measured output of each

rigid body. We have first introduced visual robotic networks consisting of the dynamics describing rigid body motion, visibility structures among bodies and visual measurements. We have then proposed a visual feedback pose synchronization law combining a vision-based observer with the pose synchronization law. Moreover, we have proved that the network with the control law achieves visual feedback pose synchronization in the absence of communication or any other measurement of the states. Finally, the experimental results have demonstrated the validity of our results.

REFERENCES

- [1] P. Ogren, E. Fiorelli and N. E. Leonard, "Cooperative Control of Mobile Sensor Networks: Adaptive Gradient Climbing in A Distributed Environment," *IEEE Trans. on Automatic Control*, Vol. 49, No. 8, pp. 1292–1302, 2004.
- [2] N. E. Leonard, D. A. Paley, F. Lekien, R. Sepulchre, D. M. Frattoni and R. E. Davis, "Collective Motion, Sensor Networks and Ocean Sampling," *Proc. of the IEEE*, Vol. 95, No. 1, pp. 48–74, 2007.
- [3] F. Bullo, J. Cortes and S. Martinez, *Distributed Control of Robotic Networks*, Princeton Series in Applied Mathematics, 2009.
- [4] Y. Igarashi, T. Hatanaka, M. Fujita and M. W. Spong, "Passivity-based Output Synchronization and Flocking Algorithm in SE(3)," *Proc. of the 47th IEEE Conference on Decision and Control*, pp. 1024–1029, 2008.
- [5] F. Chaumette and S. A. Hutchinson, "Visual Servoing and Visual Tracking," in *Springer Handbook of Robotics*, B. Siciliano and O. Khatib, eds., Springer-Verlag, pp. 563–583, 2008.
- [6] M. Sznajder, M. Ayazoglu and O. I. Camps, "Using Dynamics to Recover Euclidian 3-dimensional Structure from 2-dimensional Perspective Projections," *Proc. of the 48th IEEE Conference on Decision and Control and 28th Chinese Control Conference*, pp. 2414–2419, 2009.
- [7] M. Fujita, H. Kawai and M. W. Spong, "Passivity-based Dynamic Visual Feedback Control for Three Dimensional Target Tracking: Stability and L_2 -gain Performance Analysis," *IEEE Trans. on Control Systems Technology*, Vol. 15, No. 1, pp. 40–52, 2007.
- [8] F. Morbidi, G. L. Mariottini and D. Prattichizzo, "Observer Design via Immersion and Invariance for Vision-based Leader-follower Formation Control," *Automatica*, Vol. 46, No. 1, pp. 148–154, 2010.
- [9] P. Vela, A. Betser, J. Malcolm and A. Tannenbaum, "Vision-based Range Regulation of A Leader-follower Formation," *IEEE Trans. on Control Systems Technology*, Vol. 17, No. 2, pp. 442–448, 2009.
- [10] M. Fujita, T. Hatanaka, N. Kobayashi, T. Ibuki and M. W. Spong, "Visual Motion Observer-based Pose Synchronization: A Passivity Approach," *Proc. of the 48th IEEE Conference on Decision and Control and 28th Chinese Control Conference*, pp. 2402–2407, 2009.
- [11] T. Ibuki, T. Hatanaka, M. Fujita and M. W. Spong, "Visual Feedback Attitude Synchronization in Leader-follower Type Visibility Structures," *Proc. of the 49th IEEE Conference on Decision and Control*, pp. 2486–2491, 2010.
- [12] N. Moshtagh, N. Michael, A. Jadbabaie and K. Daniilidis, "Vision-based, Distributed Control Laws for Motion Coordination of Nonholonomic Robots," *IEEE Trans. on Robotics*, Vol. 25, No. 4, pp. 851–860, 2009.
- [13] Y. Ma, S. Soatto, J. Kosecka and S. S. Sastry, *An Invitation to 3-D Vision*, Springer, 2003.
- [14] H. Berghuis and H. Nijmeijer, "A Passivity Approach to Controller-Observer Design for Robots," *IEEE Trans. on Robotics and Automation*, Vol. 9, No. 6, pp. 740–754, 1993.
- [15] P. Barooah and J. Hespanha, "Estimation on Graphs from Relative Measurements: Distributed Algorithms and Fundamental Limits," *IEEE Control Systems Magazine*, Vol. 27, No. 4, pp. 57–74, 2007.
- [16] S. Mastellone, D. M. Stipanovic, C. R. Graunke, K. A. Inlekofer and M. W. Spong, "Formation Control and Collision Avoidance for Multi-agent Non-holonomic Systems: Theory and Experiments," *International Journal of Robotic Research*, Vol 27, No. 1, pp. 107–126, 2008.
- [17] A. Astolfi, "Exponential Stabilization of A Wheeled Mobile Robot via Discontinuous Control," *Journal of Dynamic Systems, Measurement, and Control*, Vol. 121, No. 1, pp. 121–125, 1999.